

Shock Ignition of Thermonuclear Fuel with High Areal Density

R. Betti,^{1,2} C. D. Zhou,¹ K. S. Anderson,¹ L. J. Perkins,³ W. Theobald,¹ and A. A. Solodov¹

¹Fusion Science Center and Laboratory for Laser Energetics, University of Rochester, Rochester, New York 14623, USA

²Department of Mechanical Engineering & Physics and Astronomy, University of Rochester, Rochester, New York 14623, USA

³Lawrence Livermore National Laboratory, Livermore, California, USA

(Received 6 December 2006; published 12 April 2007)

A novel method by C. Zhou and R. Betti [Bull. Am. Phys. Soc. **50**, 140 (2005)] to assemble and ignite thermonuclear fuel is presented. Massive cryogenic shells are first imploded by direct laser light with a low implosion velocity and on a low adiabat leading to fuel assemblies with large areal densities. The assembled fuel is ignited from a central hot spot heated by the collision of a spherically convergent *ignitor* shock and the return shock. The resulting fuel assembly features a hot-spot pressure greater than the surrounding dense fuel pressure. Such a nonisobaric assembly requires a lower energy threshold for ignition than the conventional isobaric one. The ignitor shock can be launched by a spike in the laser power or by particle beams. The thermonuclear gain can be significantly larger than in conventional isobaric ignition for equal driver energy.

DOI: 10.1103/PhysRevLett.98.155001

PACS numbers: 52.57.-z

In direct-drive inertial confinement fusion [1,2] (ICF), a shell of cryogenic deuterium and tritium (DT) thermonuclear fuel is accelerated inward by direct laser irradiation. As the shell stagnates, the compressed fuel is ignited from a low-density central hot spot surrounded by an ultradense shell. For ignition to occur, the alpha particle heating of the hot spot must exceed all the energy losses including expansion, heat conduction, and radiation losses. As pointed out in Ref. [3], much of the heat escaping the hot spot is deposited on the surrounding dense shell inner surface causing the ablation of the shell material into the hot spot. The ablated plasma entering the hot spot carries most of the energy lost by heat conduction back into the hot spot in the form of internal energy and pdV work. If ignition occurs, the resulting burn wave propagates from the hot spot throughout the dense fuel. Most of the fusion energy yield comes from this stage of the burn when the burning plasma core is confined for a brief time by its own inertia. The burn time depends on the dense fuel areal density ρR , and the burn-up fraction is approximately given [2] by $\theta \approx 1/(1 + 7/\rho R)$, where ρR is in g/cm^2 . The peak areal density is approximately independent of the shell implosion velocity. It increases with the laser energy and decreases with the in-flight adiabat according to the simple relation [4]

$$(\rho R)_{\text{max}} \approx \frac{1.2}{\alpha^{0.55}} \left(\frac{E_L(\text{kJ})}{100} \right)^{0.33}, \quad (1)$$

where ρR is in g/cm^2 , E_L is the UV-laser energy on target, and α is the in-flight adiabat of the inner portion of the shell. Here, the adiabat [2] is the ratio of the plasma pressure to the Fermi pressure of a degenerate electron gas. The energy gain depends on the areal density and the capsule implosion velocity. Using the direct-drive hydro-efficiency [4], the energy gain can be written as [4]

$$G \approx \frac{73}{I_{15}^{0.25}} \left(\frac{3 \times 10^7}{V_I} \right)^{1.25} \frac{\theta(\rho R)}{0.2}, \quad (2)$$

where V_I is the implosion velocity in cm/s and the laser intensity I_{15} is in units of $10^{15} \text{ W}/\text{cm}^2$. In deriving Eq. (2), it is assumed that ignition has taken place and the burn wave has propagated through the dense core. Notice that Eq. (2) indicates that the gain increases for lower implosion velocities since more mass can be assembled for the same laser energy. In addition to the high gains, massive shell implosions have good hydrodynamic stability properties during the acceleration phase. The number of e -foldings of Rayleigh-Taylor (RT) instability growth for the most dangerous modes with $k\Delta \approx 1$ (k is the mode wave number and Δ is the in-flight target thickness) is [2,4] $\gamma t \approx 0.9\sqrt{\text{IFAR}_{\text{max}}}$, where IFAR is the in-flight aspect ratio [2] defined as the maximum value of the ratio between the shell radius and thickness. The IFAR can be approximated [4] by

$$\text{IFAR}_{\text{max}} \approx \frac{51}{\langle \alpha \rangle^{0.6}} \left(\frac{V_I(\text{cm/s})}{3 \times 10^7} \right)^2 \frac{1}{I_{15}^{4/15}}, \quad (3)$$

where $\langle \alpha \rangle$ is the average in-flight adiabat. Thus, low IFAR implosions are not significantly affected by the RT instability. However, low IFAR implosions are difficult to ignite since the energy required for conventional ignition scales approximately [4,5] as $E_{\text{kin}}^{\text{ign}} \sim \text{IFAR}^{-3}$ for a fixed laser intensity. Thus, while low-adiabat low-velocity implosions have the potential for high gains, their hot-spot energy is not enough to trigger ignition. The conventional inertial fusion assembly of the hot spot and surrounding dense fuel is isobaric [6] with the plasma pressure approximately uniform throughout the entire core (Fig. 1). Both the low-density central hot spot and the high density cold surrounding fuel have similar internal energy densities.

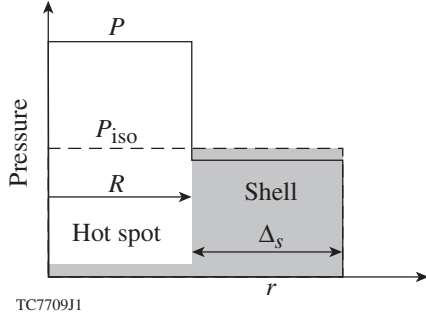


FIG. 1. Sketch of a uniform pressure *isobaric* assembly (dashed line) and of a nonisobaric assembly with the pressure peak inside the hot spot (solid line). The gray shaded region is the density profile.

However, an isobaric fuel assembly is not optimal for central ignition. Here, we show that a stagnating core with a nonuniform pressure peaked inside the hot spot has a lower ignition threshold than a uniform pressure core for the same total internal energy. We also show that such a peaked pressure profile can be attained by launching a spherically converging shock in the latest stage of the implosion. The launching time of such an *ignitor* shock must be carefully chosen. In order to maximize the hot-spot peak pressure of the final assembly, the ignitor shock must collide with the return shock inside the dense shell and near its inner surface. The return shock is the outward traveling shock driven by the rapidly increasing hot-spot pressure during the shell slowing down. The inward moving shock generated by the collision leads to a further compression of the hot spot and to a peaked pressure distribution. In this Letter, we first show that a peaked pressure profile leads to a lower ignition threshold. Then, using a simple planar hydrodynamic model, we show that a peaked pressure profile can be attained by launching a shock at the appropriate time. Finally, we use ICF hydrocodes to simulate realistic implosions with ignitor shocks. We consider the assembly in Fig. 1, and use the hot-spot model of Ref. [3]. We assume that heat conduction losses are fully recycled into the hot spot and derive the ignition conditions by balancing the alpha heating with the radiation and expansion losses. The latter represent the transfer of the hot-spot internal energy into the rebounding shell kinetic energy [3,7]. The radiation losses are retained since the capsules considered here have low implosion velocities ($V_I < 3 \times 10^7$ cm/s) leading to relatively cold hot spots. Defining with R the hot-spot radius, assuming that the pressure p is uniform within the hot spot, and using the volume average operator $\langle \rangle \equiv 3 \int_0^1 x^2 dx$ with $x = r/R$, the ignition condition can be written in the following simple form

$$P_\alpha > P_{\text{exp}} + P_{\text{rad}} \quad (4)$$

$$\frac{P_\alpha}{U} \sim p \left\langle \frac{\sigma v}{T^2} \right\rangle, \quad \frac{P_{\text{exp}}}{U} \sim \frac{1}{\tau_{\text{dec}}}, \quad \frac{P_{\text{rad}}}{U} \sim p \left\langle \frac{1}{T^{3/2}} \right\rangle, \quad (5)$$

where $U \sim pR^3$ is the internal energy and τ_{dec} is the

decompression time. Following Ref. [3], the decompression time scales as $\tau_{\text{dec}} \sim \sqrt{M_{\text{shell}}/pR}$, where M_{shell} is the shell mass. Using Eq. (2.2) of Ref. [2] for the radiation power density and combining the alpha heating and the radiation losses leads to

$$P_\alpha - P_{\text{rad}} \sim p^2 R^3 T_0^\beta [1 - (T_*/T_0)^{\beta+3/2}], \quad (6)$$

where T_0 is the central temperature for the profile [3] $T = T_0(1 - x^2)^{2/7}$ and $T_* \approx 6.4$ keV is the critical value of the central temperature corresponding to the balance of the alpha heating and radiation losses. If a fraction of the radiation losses is reabsorbed or recycled into the hot spot, the critical temperature T_* decreases with $T_* \approx 5$ keV for a 50% recycling. The parameter β comes from the power-law approximation of $\sigma v/T^2 \sim T^\beta$. Since we are considering ignited hot spots, the parameter β is chosen to optimize the power-law fit of $\sigma v/T^2$ for central temperatures exceeding T_* . We consider central temperatures ranging from 5 to 15 keV, and approximate the volume-averaged alpha heating term $\langle \sigma v/T^2 \rangle$ with a power law of the central temperature T_0^β with $\beta \approx 1$ and an error $\leq 13\%$. Substituting Eq. (6) into (4) yields the ignition condition

$$(p/R)M_{\text{shell}}T_0^2[1 - (T_*/T_0)^{2.5}]^2 > \text{const}. \quad (7)$$

Though Eq. (7) is valid for an arbitrary fuel assembly, it is convenient to introduce the parameters $\hat{\Phi} \equiv pR_{\text{iso}}/p_{\text{iso}}R$ and $\hat{\delta} \equiv T_0/T_0^{\text{iso}}$, where iso indicates an isobaric fuel assembly (Fig. 1). The ignition condition can be simplified by setting $M_{\text{shell}} \sim \rho_s \Delta_s R^2 \Sigma$, where ρ_s and Δ_s are the shell density and thickness, and $\Sigma \equiv 1 + A^{-1} + A^{-2}/3$ with $A = R/\Delta_s$. Furthermore, using the isobaric profile, we set $M_{\text{shell}}V_I^2 \sim p_{\text{iso}}R_{\text{iso}}^3(1 + A^{-1})^3$, and rewrite the ignition condition in terms of the shell areal density $(\rho_s \Delta_s)^{\text{iso}}$ of the isobaric assembly

$$(\rho_s \Delta_s)^{\text{iso}} > \frac{\text{const}[1 - (T_*/\hat{\delta}T_0^{\text{iso}})^{2.5}]^{-1}}{\hat{\Phi}^{0.5} \hat{\delta} T_0^{\text{iso}} V_I \Psi(A)}, \quad (8)$$

where $\Psi(A) \equiv \Sigma(A)/(1 + A^{-1})^{3/2} \approx \text{const}$ for relevant values of $1 < A < 4$. The parameters $\hat{\Phi}$ and $\hat{\delta}$ represent the nonisobaric modifications of the ignition condition. If the nonisobaric assembly is achieved through an adiabatic compression of the hot spot ($pR^5 = \text{const}$), then $\hat{\delta} \sim \hat{\Phi}^{1/3}$. The scalings of the shell areal density [4] [Eq. (1)] and temperature [8] [$T_0 \sim V_I^{1.3}/\alpha^{0.06}$] for an isobaric assembly are derived from fitting the results from over 50 simulations of optimized cryogenic implosions. Substituting ρR and T_0 into Eq. (8) yields the following final form of the ignition condition in terms of the laser energy required for ignition

$$E_L > \frac{E_{\text{ign}}^{\text{iso}}}{\hat{\Phi}^{2.5}} \left[1 - \left(\frac{V_*}{\hat{\Phi}^{0.25} V_I} \right)^{3.3} \right]^{-3} + \Delta E^{\text{n.i.}}(\hat{\Phi}), \quad (9)$$

where $E_{\text{ign}}^{\text{iso}} \sim \alpha^{1.8}/V_I^{6.9}$ is the laser energy required for high-velocity ($V_I \gg V_*$) isobaric ignition, V_* is the critical implosion velocity required to achieve $T_0 = T_*$, and

$\Delta E^{n.i.}(\hat{\Phi})$ is the additional laser energy required to generate the nonisobaric fuel assembly with $\hat{\Phi} > 1$. There are not accurate values for V_* and T_* but typically $T_* \sim 5$ keV and $10^7 < V_* < 2 \times 10^7$ cm/s. If $\hat{\Phi} = 1$, the fuel assembly is isobaric and $\Delta E^{n.i.} = 0$. This ignition model yields an isobaric ignition scaling similar to the one in Ref. [5]. Indeed, using the hydrodynamic efficiency scaling of Ref. [4], $\eta \sim V_I^{0.75}/I^{0.25}$, the ablation pressure scaling $p_L \sim I^{2/3}$ and taking the limit of $V_I \gg V_*$, the kinetic energy required for isobaric ignition $E_{\text{kin}}^{\text{iso}} = \eta E_{\text{ign}}^{\text{iso}} \sim \alpha^{1.8}/V_I^{6.1} p_L^{0.4}$ is remarkably close to the scaling [5] of conventional ICF implosions. If the peaked hot-spot pressure in the nonisobaric assembly is achieved through an adiabatic compression, then $\hat{\Phi}^{2.5} \sim (p/p_{\text{iso}})^3$. Notice that the ignition energy [Eq. (9)] is lowered significantly for a moderate increase of p (for example, $\hat{\Phi}^{2.5} \approx 5$ for $p \approx 1.7p_{\text{iso}}$). There may not be a unique approach to induce a nonisobaric assembly of the kind in Fig. 1. Here, we show that launching a shock during the final stage of the implosion and timing it with the return shock is an attractive option to generate a nonisobaric assembly. This can be shown using a simple planar model of a plasma slab compressing a lower density plasma [Fig. 2(a)]. The plasma is initially traveling towards a rigid wall at $x = 0$, with a constant velocity V_I and a uniform pressure of 50 Mbar [Fig. 2(a)]. The evolution is described by the single fluid Euler equations and the shock is driven by an applied pressure pulse on the plasma slab outer edge. We compare the compressed core for an initial velocity of $V_I = 2.5 \times 10^7$ cm/s without a shock, and the one for an initial velocity of $V_I = 2.16 \times 10^7$ cm/s with a shock. The shock-driving pulse has a pressure of 1.4 Gbar for 200 ps. The total energy with and without a shock is the same. The shock launching time of 320 ps is chosen to maximize the peak pressure in the hot spot. Figure 2(b) shows the compressed cores with and without shock. The nonisobaric core has a hot-spot pressure 70% larger than the isobaric core, and the energy used to drive the shock is only 23% of the total energy. It is important to observe that the driven shock (or *ignitor* shock) collides with the return shock inside the shell. The return shock is the outward moving shock driven by the rising pressure in the hot spot. Figure 3(a) shows the two shocks right before the collision.

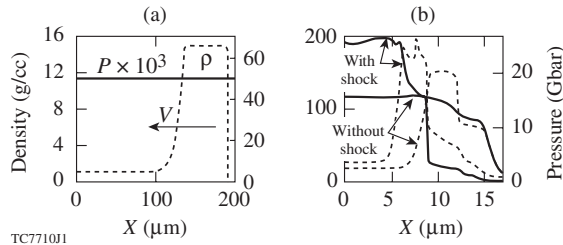


FIG. 2. Pressure (solid line) and density (dashed line) profiles of a plasma slab hitting a rigid wall. Part (a) shows the initial profiles. Part (b) shows the profiles at peak compression.

As a result of the collision, two new shocks are generated: an inward and outward moving shock [Fig. 3(b)]. It is the inward moving shock that impulsively accelerates the inner shell surface thus enhancing the piston action of the shell on the hot spot and leading to the nonisobaric assembly of Fig. 2(b). The shock-ignition technique can be used to lower the ignition energy in inertial fusion implosions. The ignitor shock can be launched by a spike in the laser power or by a particle beam, the latter being a more efficient way to drive shocks since particle beams deliver their energy directly onto the target. Existing large laser facilities such as the National Ignition Facility [9] (NIF) should be capable of testing this concept through laser-driven shocks. As an example, we consider a massive 850 μm outer radius, 343 μm -thick wetted-foam capsule [Fig. 4(a)] driven by the UV-laser pulse shown in Fig. 4(b). The implosion is simulated with the hydrocode LILAC [10]. The pulse shape [solid curve in Fig. 4(b)] consists of an adiabat-shaping [11] assembly pulse with a flattop power of 110–130 TW setting the shell on an inner adiabat $\alpha \approx 1$, average adiabat $\langle \alpha \rangle \approx 2$ and velocity $V_I \approx 2.25 \times 10^7$ cm/s. The $\text{IFAR}_{\text{max}} \approx 18$ is so low that the shell remains integral during the acceleration phase. The ignitor shock is driven by a spike in the laser power reaching 540 TW for about 100–300 ps. The fraction of absorbed power decreases from 63% during the assembly pulse to 43% during the spike. As the ignitor shock travels through the shell, its pressure increases to the Gbar level due to the shock convergence before colliding with the return shock. Because of the relatively high laser intensity $\sim 6 \times 10^{15}$ W/cm² in the spike, a significant amount of hot electrons can be generated by the laser plasma instabilities. In the simulations, we let up to 10% of the spike laser energy converted into hot electrons with a temperature of 100 keV. The hot electrons are transported to the target according to a multigroup diffusion model [10] and typically only a small fraction 5% of the hot electron energy reaches the target. A 0.5% fractional preheating during the spike is a reasonable extrapolation from the experimental results of Ref. [12]. Since the target areal density is quickly rising at the end of the pulse, hot electrons with energy ≤ 100 keV do not penetrate through the target but are stopped near the surface thus augmenting the drive for the ignitor shock. We find that the total laser energy for marginal shock ignition is 290 kJ partitioned between the

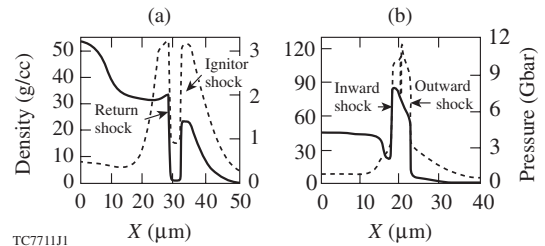


FIG. 3. Pressure (solid line) and density (dashed line) profiles for the plasma slab before (a) and after (b) the shocks' collision.

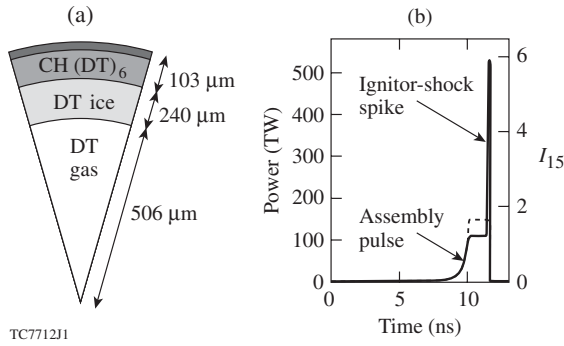


FIG. 4. Wetted-foam target (a) and 290 kJ UV-laser pulse (b) with (solid line) and without (dashed line) the shock power spike.

assembly pulse (243 kJ) and the power spike (47 kJ). The effects of the ignitor shock on the fuel assembly are shown in Fig. 5, where the pressure and density profiles at peak compression are shown for the target in Fig. 4(a) imploded by the shock-ignition pulse shape [solid curve in Fig. 4(b)] and the conventional pulse shape (dashed curve) with the same energies of 290 kJ and without alpha deposition. The nonisobaric assembly has a peak pressure 70% higher than the isobaric one, corresponding to a reduction of the ignition energy (without including the ignitor-shock energy) of $\hat{\Phi}^{2.5} \approx 4.9$ [see Eq. (9)]. Using Eq. (9), $E_L = 290$ kJ, $\Delta E_L^{n.i.} = 47$ kJ, and $\hat{\Phi}^{2.5} \approx 4.9$, we can recover the isobaric ignition energy $E_L^{iso} \approx 1.19$ MJ. We verified this result by using the hydrocode LILAC to find that marginal isobaric ignition (without the shock) for the same implosion velocity, adiabat, and intensity requires a 1.5 mm radius target and a 1.15 MJ UV-laser driver. If shock ignited with a laser energy of 310 kJ (20 kJ above the marginal energy), the target in Fig. 4 yields a 1D thermonuclear gain of 55 higher than the gain expected from the 1.5 MJ conventional direct [13] and indirect [9] drive on the NIF. However, one needs to be cautious in using the 1D results to assess the viability of this concept. Since the ignitor shock is launched at the end of the acceleration phase, the RT-amplified ablation-front perturbations are transferred by the shock from the outer to the inner shell

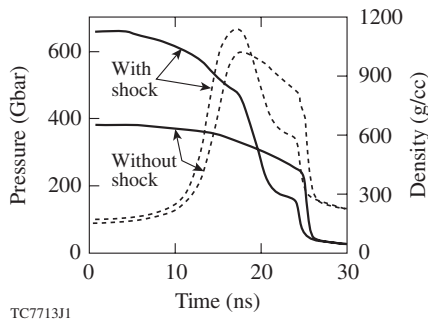


FIG. 5. Pressure (solid line) and density (dashed line) profiles at peak compression for the 290 kJ pulse shapes with and without ignitor shock.

surface, thus distorting the hot spot and possibly quenching [5,14] the ignition process. An excess energy above the marginal ignition energy of 290 kJ will be required to overcome the yield degradation due to nonuniformities. We use the 2D hydrocode DRACO [15] to simulate the implosion of the capsule in Fig. 4(a) driven by a shock-ignition UV-laser pulse of 425 kJ. The pulse has an excess energy of 135 kJ with respect to the marginal 1D value. About 275 kJ are used in the assembly pulse and 150 kJ in the shock spike. The robustness of the ignition is assessed by the size of the ignitor-shock launching window (LW) representing the time interval during which the ignitor-shock can be launched to successfully ignite the core. In 1D, the LW is about 400 ps with the gain varying from 30 for a shock launched at the early time in the LW and 60 for a shock launched at the late time in the LW. As the main source of nonuniformities, the 2D simulations include laser imprinting in accordance to the direct-drive NIF specifications [13] for the mode numbers $l \leq 100$ relevant to such thick targets. As expected, we find that laser nonuniformities do lead to a reduction of the LW size. The LW is reduced by 170 ps to 230 ps with the energy gain still about 60 for a shock launched in the late time in the LW. Similarly to fast and impact ignition [16], shock ignition is induced separately from the compression. A powerful laser pulse or particle beam can be used to drive the ignitor shock to trigger ignition at relatively low driver energies.

This work has been supported by the US Department of Energy under Cooperative Agreement No. DE-FC02-04ER54789 and No. DE-FC03-92SF19460.

- [1] J. Nuckolls *et al.*, *Nature (London)* **239**, 139 (1972).
- [2] S. Atzeni and J. Meyer-ter-Vehn, *The Physics of Inertial Fusion* (Clarendon Press, Oxford, 2004); J.D. Lindl, *Inertial Confinement Fusion* (Springer, New York, 1998).
- [3] R. Betti *et al.*, *Phys. Plasmas* **8**, 5257 (2001).
- [4] R. Betti and C. Zhou, *Phys. Plasmas* **12**, 110702 (2005); R. Betti *et al.*, *Plasma Phys. Controlled Fusion* **48**, B153 (2006).
- [5] M. C. Herrmann, M. Tabak, and J. D. Lindl, *Phys. Plasmas* **8**, 2296 (2001).
- [6] J. Meyer-ter-vehn, *Nucl. Fusion* **22**, 561 (1982).
- [7] M. Basko and J. Johner, *Nucl. Fusion* **38**, 1779 (1998).
- [8] C. Zhou and R. Betti, *Bull. Am. Phys. Soc.* **51**, 31 (2006); *Phys. Plasmas* (to be published).
- [9] S. W. Haan *et al.*, *Phys. Plasmas* **2**, 2480 (1995).
- [10] J. Delettrez and E. B. Goldman, Laboratory for Laser Energetics Report No. 36, 1976.
- [11] V. Goncharov *et al.*, *Phys. Plasmas* **10**, 1906 (2003); K. Anderson and R. Betti, *Phys. Plasmas* **11**, 5 (2004).
- [12] C. Stoeckl *et al.*, *Phys. Rev. Lett.* **90**, 235002 (2003).
- [13] P. W. McKenty *et al.*, *Phys. Plasmas* **8**, 2315 (2001).
- [14] R. Kishony and D. Shvarts, *Phys. Plasmas* **8**, 4925 (2001).
- [15] P. Radha *et al.*, *Phys. Plasmas* **12**, 032702 (2005).
- [16] M. Tabak *et al.*, *Phys. Plasmas* **1**, 1626 (1994); M. Murakami and H. Nagatomo, *Nucl. Instrum. Methods Phys. Res., Sect. A* **544**, 67 (2005).